Combined Negative Effects of Microplastics and Plasticizer DEHP: the Increased Release of Nets Delays Wound Healing

Xu Shi
Northeast Agricultural University
Wei Cui
Northeast Agricultural University
Tong Xu
Northeast Agricultural University
Xue Qi
Northeast Agricultural University
Zhiruo Miao
Northeast Agricultural University
Shiwen Xu (shiwenxu@neau.edu.cn)
Northeast Agricultural University

Research

Keywords: MPs, DEHP, Wound healing, Oxidative Stress, Nets

Posted Date: December 3rd, 2021

DOI: https://doi.org/10.21203/rs.3.rs-1100694/v1

Abstract

Introduction: Environmental pollutants microplastics (MPs) and di (2-ethyl) hexyl phthalate (DEHP) can cause damage to multiple organs by causing oxidative stress. Oxidative stress participates in the healing of skin wounds through the release of neutrophil extranets (Nets). Here, we studied the effects of DEHP and MPs on skin wound healing in mice after single and combined exposure for 1 month.

Results: The results showed that MPs delayed the healing of skin wounds, and the combination of the two delayed wound healing more significantly. The results of in vivo and in vitro experiments showed that the release of oxidative stress and Nets in the single exposure group increased, and the combined exposure group increased more. Further mechanism studies showed that the skin chemokines of the single exposure group increased, the NF-κB pathway was activated, the Wnt pathway was inhibited, and the epidermal growth factor and fibrosis-related indicators decreased. The combined exposure group showed a more obvious trend.

Conclusion: In summary, the above results indicate that DEHP combined with MPs induces an increase in the release of Nets by causing excessive skin ROS production and increases the expression of chemokines and interferes with the expression of healing factors by regulating the NF-κB and Wnt pathways.

1. Introduction

Plastic products have a sharp increase in the use of plastic products due to their cheapness and convenience. They can be broken down into small fragments through physical and chemical decomposition and become microplastics (MPs) and nanoplastics (NPs) (Yousif and Haddad 2013). However, due to irresponsible waste recycling and slow biodegradation rates, plastics have accumulated in the global environment. It has been proved that plastics have been detected in surface waters and oceans around the world (Cincinelli, Scopetani et al. 2017, Koongolla, Lin et al. 2020). Moreover, MPs particles ingested have been texted in various tissues of mammals and aquatic such as mice, fish, rats, etc. (Feng, Zeng et al. 2021, Shengchen, Jing et al. 2021, Zhang, Sun et al. 2021), even threatening the integrity of the food chain and the ultimate ability of ecosystem restoration (Thomas, Perono et al. 2021), which has caused people to worry about their environmental and human health risks. At the same time, more and more evidence indicate that MPs may cause immune and inflammatory responses, oxidative stress (Shengchen, Jing et al. 2021), abnormal changes in metabolism and even genetic damage (Thomas, Perono et al. 2021). It has been reported in the literature that the use of MPs and tributyltin (TBT) alone or combined may cause an imbalance of the intestinal flora in mice (Jiang, Yuan et al. 2021). Studies have found that PS-MPs cause excessive production of reactive oxygen species (ROS) and inhibit skeletal muscle regeneration, inhibits the myogenic differentiation of C2C12 cells, and promotes fat differentiation through increasing the level of NF-κB pathway (Shengchen, Jing et al. 2021). Di (2-ethylhexyl) phthalate (DEHP) is a plasticizer. Due to its widespread use, DEHP pollution in the environment seriously threatens the health of humans and animals (Gao, Xu et al. 2019). In the Jiulong

River Estuary in the southeastern of China, the annual DEHP concentration in water ranges from 0.12 to 12.4 mg/L. DEHP is one of the main components of PAE distribution in water (Li, Liang et al. 2017). Although a large number of MPs and DEHP are removed from the final effluent of the sewage treatment plant, MPs (2.419×10 MP/d) and DEHP still enter the water environment every day, posing a threat to the health of fish and local residents (Takdastan, Niari et al. 2021). Human and animal exposure to DEHP through ingestion, inhalation and skin absorption can cause liver and kidney damage (Camacho, Latendresse et al. 2020), male and female reproductive disorders and developmental toxicity (Wang, Tian et al. 2021). In addition, it is reported that DEHP induces the formation and apoptosis of carp neutrophil extracellular traps (Nets) by promoting ROS burst and autophagy (Yirong, Shengchen et al. 2020). DEHP can cause the production of ROS in HMC-1 cells, the activation of NF-κB pathway, and the regulation of COX-2 and IL-1β expression (Oh, Lim et al. 2010). There are data showing that MPs and DEHP inevitably have the risk of simultaneous exposure to humans and animals in the ecological environment (Takdastan, Niari et al. 2021). Therefore, carrying out relevant research on MPs and DEHP is of great significance to the protection of biodiversity and human food security.

The skin is the body's first line of defense against injury and infection. When the skin is damaged, a series of complex and coordinated processes will occur in the body, involving various cellular components including inflammatory cells and tissue repair cells. And pathways such as TGFβ and Wnt also promote the healing of skin wounds (Gos, Miłoszewska et al. 2009, Yang, Tsai et al. 2017). Zinc oxide nanoparticles (ZnO NPs) affect psoriasis-like lesions and promote inflammation and keratinocyte apoptosis through p-NFκB p65 (Lai, Wang et al. 2021). As we all know, inflammation is one of the typical features of the wound healing process, and neutrophils are quickly recruited to the wound bed and participate in the early stages of wound healing (Wong, Demers et al. 2015). Some studies have found that neutrophils migrate to the wound site and can form a Net (Martin and Leibovich 2005). It is worth noting that in a variety of pathological conditions, the increase of Nets has been shown to impair wound healing (Wang and Jing 2018). Nets delayed peptidyl arginine deiminase-4 (PAD4)-mediated the healing of skin wound in diabetic mice (Wang and Jing 2018). Nets formation requires the production of ROS. ROS stimulates Nets to activate PAD4, and then leads to the citrullination of histone H3 (Cit H3), thereby activating neutrophil elastase (NE) and the migration and processing of myeloperoxidase (MPO) (Wang, Zheng et al. 2018, Zheng, Wang et al. 2020). Bongkrekic acid (BKA) increases the production of ROS in neutrophils, and PAD4 and P2X1 receptors also mediate the formation of Nets triggered by BKA (Zhou, Sun et al. 2021). Fumonisin B (FB) induces the formation of Nets, increases ROS levels, and reduces SOD and CAT activities (Wang, Liu et al. 2020). It has been reported that chronic low-dose $CdCl_2$ exposure reduces neutrophil infiltration by inhibiting the expression of chemokines, and inhibits the expression of pro-inflammatory cytokines, thereby impairing skin wound healing (Mei, Yao et al. 2017). Nutritional deficiency diseases such as selenium deficiency can increase the number of chicken neutrophils by increasing the expression of chemokines, and induce the increase of Nets through ROS bursts, which can cause arteritis (Chi, Zhang et al. 2021). The above studies have shown that the wound healing process involves the recruitment of neutrophils, the burst of ROS, and the formation of Nets, which may be accompanied by inflammation.

In summary, too many Nets in the tissues can cause excessive local inflammation, leading to delayed wound healing. DEHP can lead to the release of Nets caused by ROS bursts (Yirong, Shengchen et al. 2020). Exposure to MPs can cause oxidative stress and inflammation (Shengchen, Jing et al. 2021). Due to the influence of daily necessities and industry, poisons in the environment often appear at the same time (Zhang, Lin et al. 2021, Zhang, Wang et al. 2021), DEHP and MPs may be exposed at the same time (Takdastan, Niari et al. 2021). Therefore, we have reason to doubt whether the combined exposure of MPs and DEHP has any effect on skin wound healing in mice, and whether ROS/Nets and NF-κB/Wnt pathways are involved in this wound healing process. In this study, mice were used as the research object to establish a skin trauma model after 1 month of MPs exposure, DEHP exposure and dual exposure. Then we used H&E staining, Masson staining and Immunofluorescence to determine the formation of the Nets and wound healing. In addition, we detected the expression levels of wound skin inflammatory factors, Wnt pathway, TGFβ pathway and healing factors. The effects of MPs and DEHP on the formation of Nets were detected in vitro. This study purposes to proclaim the mechanism which synergy of DEHP and MPs to cause delayed wound healing through the increasing release of Nets. It will provide new views into the toxicology research of DEHP and MPs and the treatment of wound healing diseases.

2. Results

2.1 DEHP combined with MPs delays the healing of skin wounds

According to the pictures of wound healing, it can be directly observed that DEHP and MPs can cause the delay of wound healing compared with the control group. Surprisingly, the wound healing was the worst in the DEHP+MPs group (Fig. 1a). In addition, the wound regeneration rate further showed that the control group healed 90%, MPs and DEHP healed about 40% and 60%, while the DEHP+MPs group only healed less than 20% (Fig. 1b) ($p<0.05$). In addition, the weight ratio before and after the establishment of the trauma model was analyzed, and it was found that the ratio of the DEHP+MPs group increased (Fig. 1c) ($p<0.05$), indicating that the skin trauma caused the mice to lose weight when DEHP and MPs were exposed together.

H&E staining showed that the wound in the control group was basically healed, the boundary between the disease and healthy was gradually blurred, and the epidermal hair follicle was regenerated well (red arrow) (Fig. 1d). Masson staining also confirmed that the healed wound was filled with a large amount of collagen fibers, and under a 10X microscope, it was also found that the muscle layer of the wound was regenerated from the edge (yellow arrow) (Fig. 1e). In the DEHP group, the boundary between disease and health was obvious, with slight inflammatory cell infiltration, but the skin wound was basically healed, hair follicles began to form, and the magnification revealed that the muscle tissue was not significantly regenerated (Fig. 1d). Combined with Masson staining, it was found that most of the wound was filled with fibrotic collagen fibers (black arrow) (Fig. 1e). A large crust was seen in the MPs group, the wound was in the initial stage of healing, and the bottom of the wound was regenerated obviously (green arrow)

(Fig. 1d). And Masson staining also found that there is slight fibrosis here, and fibrosis and inflammatory cell infiltration are obvious at the junction of disease and health (Fig. 1e). In the DEHP+MPs group, fibrosis and inflammatory cell infiltration occurred at the junction of disease and health, and fibroblasts proliferated, but there was no obvious healing at the skin wound, only a thin layer of crust (Fig. 1d, 1e). In short, H&E and Masson staining show that, compared with the control group, DEHP mainly delayed the muscle regeneration in the healing wound, and the fibrosis was no different from the control group. The skin wound regeneration in the MPs group was slow, and the fibrosis was milder than that in the control group and the DEHP group. The skin wounds in the DEHP+MPs group did not heal, and the degree of fibrosis was the lowest among the four groups.

2.2 Effects of DEHP and MPs on skin oxidative stress and neutrophil ROS production

Since oxidative stress can induce the formation of Nets, we first texted the superoxide production and antioxidant enzyme activities during skin wound healing under DEHP and MPs exposure. As shown in Figure 2a, both DEHP and MPs can significantly inhibit the activities of SOD and CAT, which were the major antioxidant enzymes. And the activity of enzymes involved in free radical reactions (GSH and GSH-Px) decreased, the content of H_2O_2 and MDA increased, and the activity of T-AOC decreased ($p<0.05$). At the same time, the DEHP+MPs group showed more obvious effects ($p<0.05$), indicating that the aggravating effect of oxidative stress was more obvious. Furthermore, the results demonstrated the changes in ROS production levels of neutrophils stimulated by DEHP and MPs in vitro ($p<0.05$). In order to detect the recruitment of neutrophils in skin wounds, we tested the expression levels of 6 chemokines (CCL1, CCL4, CCL17, CXCL12, CXCL13 and CXCL14). The results showed that in addition to CCL1 and CXCL13 DEHP group showed a downward trend, the other MPs group and DEHP+MPs group showed an upward trend (Fig. 3b). This shows that MPs induce increased recruitment of neutrophils in skin wounds, and DEHP combined with MPs aggravates this phenomenon. Both the fluorescence microscope (Fig. 2c) and the fluorescence microplate reader (Fig. 2d) observed that MPs and DEHP significantly increased the production of ROS in neutrophils, while the ROS level in the DEHP+MPs group further increased ($p<0.05$). These results indicate that DEHP and MPs can induce overproduction of ROS, and the combination of the two makes ROS reach higher levels.

2.3 Effects of DEHP and MPs on the recruitment of neutrophils and the formation of Nets in mouse skin

Then in order to detect the formation of Nets, we detected the expression of Nets markers. The results showed that the fluorescence intensity of MPO and Cit H3 in mouse skin wounds increased significantly with the exposure of DEHP or MPs (Figure 3a, 3b), and the DEHP+MPs group made the fluorescence intensity reach another height. In view of the net appearance of Nets, we counted Merged graphs and found that the number of Nets in the DEHP group and MPs group increased, while the DEHP+MPs group further increased (Figure 3c) ($p<0.05$). We also found that the exposure of DEHP or MPs induced an up-

regulation of Cit H3, NE, MPO and PAD4 mRNA levels, and the combined treatment of DEHP and MPs further up-regulated (Fig. 3d) ($p<0.05$). The western blot results also added that the DEHP and MPs combined treatment group Nets marker NE, Cit H3 and MPO protein expression levels were the highest (Fig. 3e) ($p<0.05$). The above results indicate that DEHP promotes the increase in the formation of Nets in the wounded skin of mice induced by MPs.

2.4 Effect of DEHP and MPs on the formation of Nets of isolated neutrophils in vitro

In order to verify the effect of DEHP and MPs on the formation of Nets in vitro, we extracted neutrophils from the peripheral blood of mice through a kit. Compared with the control group, we observed that the DEHP group had very few Nets formation through scanning electron microscopy (Fig. 4a). In the MPs group, we not only saw the basic morphology of MPs (1-10μm in diameter), but also observed that neutrophils adhered to the surface of MPs and formed obvious Nets. It is worth noting that DEHP+MPs were showing more Nets release (Fig. 4a). In addition, we performed Sytox Green staining on the neutrophils and found that compared with the control group, there was very little green filamentous fluorescence (red arrow) in the DEHP group (Fig. 4b). The green filamentous fluorescence in the MPs group was relatively more, and the DEHP+MPs group showed a lot of green filamentous fluorescence, which was comparable to the positive control group (PMA group). By detecting the expression levels of Nets components (NE, Cit H3, MPO and PAD4) in neutrophils, we found that DEHP and MPs induced a significant rise in the levels of Cit H3 and NE ($p<0.05$), while the expression changes of MPO and PAD4 were not significantly different in Fig. 4c ($p>0.05$). It is worth noting that the mRNA and protein standards of NE, H3, MPO and PAD4 in the DEHP+MPs group were significantly increased ($p<0.05$), which were at least two times higher than the control group (Fig. 4d). The above results indicate that single exposure induces an increase in the release of Nets, but the combined treatment of DEHP and MPs makes the release of Nets more significantly increased.

2.5 Effect of excessive release of Nets on inflammation

We further tested the expression changes of NF-κB inflammation pathway genes (NF-κB, COX-2, TNF-α, iNOS and PTGEs) and ILs (IL-1β, IL-6, IL-8 and IL-10) inflammatory factors, which reflects the influence of inflammatory factors released by Nets on the NF-κB inflammatory pathway. We found that DEHP or MPs caused inflammation in the wounds of mice, which was manifested by the upregulation of NF-κB pathway related genes, IFN-γ, IL-1β, IL-6 and IL-8 in the DEHP and MPs groups, while the downregulation of IL-10 (Figure 5a, 5c) ($p<0.05$). However, the protein level of IL-10 in the MPs group did not change significantly ($p>0.05$). In addition, under the co-stimulation of DEHP and MPs, the level of inflammation further increased, manifested by changes in the mRNA levels (Figure 5a) and protein levels (Figure 5b, 5c) of the interleukin and NF-κB pathway related genes ($p<0.05$). The above results indicate that DEHP or MPs can cause Nets-mediated skin wound inflammation in mice, and DEHP can exacerbate the inflammatory effect of MPs.

2.6 Effect of excessive inflammation on Wnt pathway, TGFβ pathway and EGF expression

Due to the important role of Wnt pathway in fibrosis healing, we analyzed the mRNA and protein levels of Wnt pathway (Wnt, GSK-3β and β-catenin). We discovered that DEHP or MPs treatment significantly reduced the levels of Wnt and β-catenin, and significantly increased the level of GSK-3β (Fig. 6a, 6b) ($p<0.05$). The DEHP+MPs dual treatment group exacerbated the changes in these genes. Then, we detected the expression level of TGFβ pathway, which is closely related to fibrosis and healing. Immunofluorescence results showed that compared with the control group, DEHP or MPs treatment reduced the fluorescence intensity of TGFβ and α-SMA to varying degrees, while the fluorescence intensity of the combined treatment group further decreased (Fig. 6c). The mRNA and protein results of TGFβ and α-SMA also corresponded to the immunofluorescence results (Fig. 6d, 6g). In addition, we also found growth promoting factor 1 (IGF-1), keratinocyte growth factor (KGF), platelet-derived growth factor (PDGF), basic fibroblast growth factor (bFGF), type I collagen (Col1) and type III collagen (Col3) levels were significantly lower than the single exposure group (Figure 6e) ($p<0.05$). Then we also found that single exposure resulted in the downregulation of epidermal growth factor (EGF) (Figure 6c, 6f, 6g). DEHP combined with MPs reduced the expression of EGF to the lowest value among the four groups, which coincided with the appearance of skin healing. The expression level of bFGF also corresponded to the level of EGF (Fig. 6e, 6g). Moreover, we also compared the mRNA levels of two EGFs (vEGF and bEGF) and found that DEHP and MPs have a significant effect on the expression of vEGF (Fig. 6f) ($p<0.05$). These findings indicate that DEHP or MPs inhibit the TGFβ and Wnt pathway and reduce the level of EGF. The combined treatment of DEHP and MPs will exacerbate this phenomenon.

3. Discussion

Although some studies have found that exposure to MPs and DEHP can cause immune dysfunction, most studies have focused on aquatic animals or exposure alone. It is well known that the healing of skin wounds is also closely related to immune function. In previous studies, it has been determined that neutrophils play a vital role in wound healing. It has been reported that the excessive release of Nets can delay skin healing (Lämmermann, Afonso et al. 2013). Based on this, this study explored the effects of MPs and DEHP exposure alone or combined on skin wound healing in mice, as well as the effect of NETs on skin healing in this case. The results found that single or combined exposure caused the detention of skin wound healing, different degrees of oxidative stress, the increasing of chemokines, the increasing of Nets release, the activating of NF-κB pathway, the inhibiting of TGFβ and Wnt pathways, and the decreasing of EGF expression.

Previous in vitro experiments have found that DEHP induces the formation of carp Nets by promoting the burst of ROS (Oh, Lim et al. 2010, Yirong, Shengchen et al. 2020). In vivo and in vitro, MPs significantly increased the production of oxidative stress and ROS respiratory bursts in mice (Shengchen, Jing et al. 2021). In the current study, in vivo results found that DEHP or MPs treatment obviously reduced the

activities of GSH, GSH-Px, T-AOC, CAT and SOD, and rised the content of H_2O_2 and MDA in skin trauma, illustrating that oxidative stress has occurred. At the same time, in vitro experiments have also confirmed this phenomenon. It is important that the generation of ROS in neutrophils is a prerequisite for stimulating the release of Nets(Wang, Zheng et al. 2018, Zheng, Wang et al. 2020). We found that the expression of Nets formation markers (NE, MPO, Cit H3 and PAD4) in the skin of trauma exposed to DEHP or/and MPs were up regulated. In vitro DEHP or MPs treatment found that MPs exposure induced the formation of Nets, and the joint treatment of DEHP and MPs aggravated this response. And the mRNA and protein levels of Nets markers show the same trend as in vivo experiments. Our experiments confirmed for the first time that both in vivo or in vitro exposure of MPs can cause the release of NETs, and combined exposure to DEHP can aggravate this phenomenon. The increase of chemokines in the tissue can promote the recruitment of neutrophils (Papayannopoulos and Venizelos 2017). Our research found that MPs can up-regulate the mRNA levels of chemokines. DEHP will cooperate with MPs to further up-regulate the expression of chemokines. Studies have found that selenium deficiency recruits neutrophils by up-regulating the expression of chemokines in arterial tissues and promotes the formation of Nets (Chi, Zhang et al. 2021). In addition, studies have found that CXC chemokines can activate and attract neutrophils to the inflammation site of the mouse cremaster muscle (Zhang, Liu et al. 2001). These results reflect that DEHP combined with MPs exposure first recruits more neutrophils to the wound by up-regulating the level of chemokines, while dual exposure stimulates the release of Nets by aggravating oxidative stress. Therefore, the two pathways working at the same time allow us to discover that the dual exposure of DEHP and MPs leads to excessive activation of Nets in the skin wound.

Recently, the downside of excessive activation of Nets, that Nets may be the center of the vicious circle of inflammation when inflammation occurs, has gradually been revealed (Chi, Zhang et al. 2021). Previous studies have shown that excessive release of Nets will increase NF-κB activation (Zhu, Zhang et al. 2021). In addition, the increase of Nets in the serum of patients with atherosclerosis (AS) exacerbates the progression of atherosclerosis (An, Li et al. 2019). NF-κB pathway is a classic pathway of inflammation, and its downstream includes COX-2, TNF-α, iNOS, PTGEs and other genes; The activation of NF-κB up-regulates the mRNA levels of IL-1β, IL-6, IL-8 and down-regulates IL-10 expression (Shi, Wang et al. 2020). This experiment found that DEHP or MPs exposure induce the activation of the NF-κB inflammatory pathway, and it is worth noting that DEHP combined with MPs have a more obvious inflammatory effect on skin wounds. The Wnt pathway can promote cell proliferation, regulate the EMT signal pathway and the process of fibrosis (Zhang, Geng et al. 2021). Studies have found that the crosstalk between Wnt and NF-κB pathway was conducive to the development of apical periodontitis (AP) (Guan, He et al. 2021). In this experiment, we found that the Wnt pathway of normally healed wounds was activated, and DEHP or/and MPs exposure caused the Wnt pathway to be inhibited to varying degrees, which was manifested by the down trend of Wnt and β-catenin and the rise trend of GSK-3β. It has been reported that TGF-β, α-SMA, IGF-1 and EGF play pivotal roles in wound healing, and the better the skin healing, the higher the expression of these factors (Cheng, Lv et al. 2021, Karim, Alkreathy et al. 2021). In the process of wound healing, the Wnt/β-catenin pathway is activated and further increases the secretion of growth factors such as IGF-1 and TGFβ, which may be involved in the tissue remodeling process (Kim, Shin et al. 2021).

In this experiment, we first found through immunofluorescence staining that DEHP or/and MPs reduced the expression of EGF, a factor that reflects epidermal regeneration. And the expression of TGFβ, α-SMA and healing-related factors also changed accordingly. It shows that the Wnt pathway is involved in regulating the expression of IGF-1, EGF, TGFβ, KGF, PDGF, bFGF and other growth factors to affect the healing of skin wounds. It is worth noting that the combined exposure of DEHP and MPs has a more significant decrease in expression level than other groups. The above results indicate that excessive inflammatory response inhibits the Wnt pathway is the mechanism of delayed skin wound healing.

In conclusion, we found that the combined effects of DEHP and MP caused delayed skin wound healing in mice. In terms of mechanism, DEHP promotes MPs-induced overproduction of ROS and increased levels of chemokines in wound tissues, thereby stimulating increased Nets release, and interferes with the regulation of healing factors by regulating the expression levels of NF-κB and Wnt pathways. In short, plasticizers DEHP and MPs delay skin wound healing by increasing the release of Nets. The results of this experiment are of great value for revealing the combined toxicity of MPs and DEHP, expand the field of MPs toxicology research, and provide a reference for the toxicology research of mammalian wound healing.

4. Materials And Methods

4.1 Animal grouping and trauma model establishment

SPF-grade male Kunming mice (mass 20-25 g, about 6 weeks old) were provided by Harbin Medical University Experimental Animals. The indoor air is fresh, 75%±5% relative humidity, suitable temperature, and free supply of water and feed (Shenyang Changsheng provides standard pellet feed). Observe all experimental animals for one week and carry out follow-up tests after there is no death or mental abnormality. Forty 6-week-old mice were stochastically separated into Control group, DEHP group, MPs group and DEHP+MPs group (n=10). The control group had normal diet and drinking water. MPs (Mingshuo Chemical Company, China) were added to the drinking water (0.1 g/L) of the MPs group and DEHP+MPs group, and the water was mixed 3 times a day. In the DEHP group and the DEHP+MPs group, DEHP (Solarbio, SD9580) was added to the feed at a dose of 200 μM/kg, while the control and MPs group were given the same amount of corn oil (solvent). All groups of food and drinking water were free to eat. The whole process lasted for four weeks and then the mouse skin injury model was constructed.

Use isoflurane (EZVET, China) to perform inhalation anesthesia on mice, and the anesthesia time does not exceed 30 s. We shaved off the hair on the back of the mouse and used a skin punch and scissors to cut out a round full-thickness skin with a diameter of 6 mm ± 1 mm. One week after the wound was healed, the mice were euthanized by isoflurane inhalation. One portion was fastened in 4% neutral formalin (Biosharp, China) for H&E staining, Masson staining and Immunofluorescence. Another portion of the skin wound was taken out and stored at -80°C for future use.

4.2 Cell separation, extraction and treatment

The mice were inhaled anesthetized with isoflurane for 30 s, then opened the chest cavity of the mice with clean scissors and tweezers and used a 5 mL syringe (pre-filled with 0.6 mL anticoagulant, TBDTM-0050) for cardiac blood sampling. Then, we used the mouse peripheral blood neutrophil extraction kit (TBD, China) to isolate neutrophils according to the instructions. The medium ratio of neutrophils is 90% RPMI-1640 (Gibco, USA), 10% fetal bovine serum (FBS; BI, Italy) and 1% penicillin-streptomycin-amphotericin B (Beyotime, China). The neutrophils were cultured in a humidified 37°C incubator with 5% CO_2. We used the trypan blue method to determine the survival rate of isolated neutrophils, which exceeded 95%. In addition, we made cell smears and checked the purity of neutrophils with Giemsa staining, which exceeded 99%.

Freshly isolated primary neutrophils were cultured for 2 h, then DEHP and MPs were added to the DEHP group, MPs group and DEHP+MPs group at 400 μM and 0.1 mg/L and cultured for 6 h. If PMA is added for stimulation, we need to add 500 nM PMA for 3 h after adding DEHP or MPs for 3 h.

4.3 Histologic preparation and assessments

In order to reveal the internal mechanism of the pathological changes and delayed healing of MPs and DEHP on the wound healing, we performed the following histological examination on the wound site of mice. The skin of mice was fixed with 4% paraformaldehyde for at least 24 h. Then, the skin tissues of each group were evenly embedded in 3 parallel specimens in liquid paraffin, and after cooling, 3 sections (4 μm) (n=3) were made on a microtome (Leica, Germany). As the method described by the predecessors (Chi, Zhang et al. 2021), we performed H&E and Masson staining on the slices of each group of wounded skin. For the immunofluorescence staining of wounded skin, as previously described (Shengchen, Jing et al. 2021), perform immunofluorescence staining of MPO, Cit H3, TGFβ, α-SMA and EGF. Finally, we control the color development time to observe and collect images using a fluorescence microscope (Nikon, Japan), and use Image J to quantify the fluorescence intensity.

4.4 Scanning electron microscopy

Neutrophils were inoculated on polylysine-coated cell slides (Liangyi Biotech, China), treated according to the dose in section 2.2, and finally fixed with 2.5% glutaraldehyde at 4°C overnight. According to the way described by the predecessors, we used the scanning electron microscope to observe the formation of the mesh (Yin, Yang et al. 2019). We used a scanning electron microscope (SU-8010, Hitachi Ltd., Tokyo, Japan) to magnify 8000× to take pictures.

4.5 Detection of oxidative stress in mice skin

The skin tissues of each group were homogenized in 0.9% saline, and the supernatant was centrifuged for the detection of the oxidative stress kit. We used Coomassie Brilliant Blue Method to determine protein concentration. MDA, GSH, H_2O_2, GSH-Px, SOD, CAT and T-AOC detection kits were all purchased from Nanjing Jiancheng Institute of Biological Engineering. SOD activity, xanthine oxidase method; GSH-PX and GSH activity, 5'5-dithio-nitrobenzoic acid color method; MDA content, thiobarbituric acid method: CAT activity, molybdate ammine complex Compound method; T-AOC, phenanthline complex method.

4.6 ROS detection

According to the method stated in Song's paper (Song, Li et al. 2021), we used a reactive oxygen kit (Nanjing Jiancheng, China) to fluorescently label the respiratory bursts of neutrophils in the four treatment groups to analyze the generation of ROS. Transfer 100 μL of PBS containing neutrophils to a 96-well plat and use an Infinite M200® plate reader (TECAN, Switzerland) to detect the fluorescent signal. Then we obtained ROS images of neutrophils through a fluorescence microscope (Thermo Fisher Scientific, USA).

4.7 Fluorescence microscopy assessment of NETs

We first put poly-L-lysine-coated glass slides in a 24-well plate, planted neutrophils (10^5 cells), and then let it stand at 37°C for 2 h. Then perform grouping processing as described in section 2.2. Washing twice with PBS, and then incubate with 5 μM Sytox Green stain (Invitrogen, USA) and 5 μM DAPI stain (Beyotime, China) for 30 min. After washing twice with PBS, it was covered with anti-fluorescence mounting tablets (Beyotime, China). A fluorescence microscope (EVOS FL Auto, Life Technologies, MD, USA) was used to evaluate the formation of Nets.

4.8 RNA preparation and RT-PCR in tissue and cell

We use RT-PCR to detect the mRNA expression of target genes in skin tissues and neutrophils. As mentioned before (Shengchen, Jing et al. 2021), Trizol (Takara, Japan) was used to extract total RNA from mouse skin tissues and neutrophils according to the manufacturer's instructions. When the A260/A280 of total RNA is between 1.9-2.1 and the concentration is >350 ng/μL, we used cDNA first-strand synthesis kit (Bioer, China) and Real Time PCR Kit (Bioer, China) for reverse transcription and fluorescence quantification of total RNA from wounded skin and neutrophils. The mRNA primer sequence used in the experiment was synthesized by Shanghai Shenggong (Table 1). The GAPDH sequence was used as a standardized endogenous control. The $2^{-\Delta\Delta CT}$ method was used to calculate the expression level of target mRNA relative to GAPDH.

Table 1
Gene primers used in real-time PCR

Gene	Forward Primer (5′-3′)	Reverse Primer (5′-3′)
CCL1	CATGATGGTGGCTGTTATCTTG	CAAGAAGCTGAAACGAACTTCA
CCL4	CTCAGCTCTGTGACTACATCAA	GAAGAGACCTGAGGGAATCTTC
CCL17	GATTACTTCAAAGGGGCCATTC	GCCTTCTTCACATGTTTGTCTT
CXCL12	TCTGAAAATCCTCAACACTCCA	CAGGTACTCTTGGATCCACTTT
CXCL13	TTGTGATCTGGACCAAGATGAA	GACTTTTGCTTTGGACATGTCT
CXCL14	AGGAGAAGATGGTTATCGTCAC	GGCATTGTACCACTTGATGAAG
NE	CTGTGTGAACGGCCTAAATTTC	CAGAGAAGGTCTGTCGAGTG
MPO	CAGGAACAACATCACCATTCG	CTTGGAAGCGTGTATTGATAGC
CitH3	CTTTAAGACGGACCTGCGCTTCC	GCTGGATGTCCTTGGGCATAATGG
PAD4	GACCCGAAAGCTCTATATGTCA	TATTCCCGATGAGAATTCTGCC
IL-1β	CACTACAGGCTCCGAGATGAACAAC	TGTCGTTGCTTGGTTCTCCTTGTAC
IL-6	CTCCCAACAGACCTGTCTATAC	CCATTGCACAACTCTTTTCTCA
IL-8	GGGCTGCATCTAAAGTAAATGG	CAGAACACTGCTGTAGAAGGTA
IL-10	TTCTTTCAAACAAAGGACCAGC	GCAACCCAAGTAACCCTTAAAG
TNF-α	ATGTCTCAGCCTCTTCTCATTC	GCTTGTCACTCGAATTTTGAGA
iNOS	ATCTTGGAGCGAGTTGTGGATTGTC	TAGGTGAGGGCTTGGCTGAGTG
NF-κB	CAAAGACAAAGAGGAAGTGCAA	GATGGAATGTAATCCCACCGTA
COX-2	ATTCCAAACCAGCAGACTCATA	CTTGAGTTTGAAGTGGTAACCG
PTGEs	CTCCAGTATTACAGGAGTGACC	TGAGGACAACGAGGAAATGTAT
TGFβ	CCAGATCCTGTCCAAACTAAGG	CTCTTTAGCATAGTAGTCCGCT
α-SMA	CATCAGGGAGTAATGGTTGGAATGGG	GTGTTCTATCGGATACTTCAGCGTCAG
EGF	ACAGAAGGAGTAGATACGCTTG	GATTATTCGATGATGCTTCCCG
vEGF	TAGAGTACATCTTCAAGCCGTC	CTTTCTTTGGTCTGCATTCACA
bEGF	CATCAAGCTACAACTTCAAGCA	CCGTAACACATTTAGAAGCCAG
IGF1	GAGGGGCTTTTACTTCAACAAG	TACATCTCCAGTCTCCTCAGAT
Wnt	GGGTTTCTACTACGTTGCTACT	CAGACTCTTGGAATCCGTCAA
GSK-3β	TGGTAGCATGAAAGTTAGCAGA	CTCTCGGTTCTTAAATCGCTTG

Gene	Forward Primer (5′-3′)	Reverse Primer (5′-3′)
β-catenin	CTGCTGTCCTATTCCGAATGTCTGAG	GGCACCAATGTCCAGTCCAAGATC
bFGF	AGTTGTGTCTATCAAGGGAGTG	CATTGGAAGAAACAGTATGGCC
KGF	GAGCGACACACAAGAAGTTATG	CATCTCTTGGGTCCCTTTTACT
PDGF	GTCCAGGTGAGAAAGATTGAGA	GTCATGGGTGTGCTTAAACTTT
Col1	TGAACGTGGTGTACAAGGTC	CCATCTTTACCAGGAGAACCAT
Col3	GAAAGAATGGGGAGACTGGAC	TACCAGGTATGCCTTGTAATCC
GAPDH	CCCAGAAGACTGTGGATGG	ACACATTGGGGGTAGGAACA

4.9 Western blot analysis in skin tissues and neutrophils

Extract protein from skin tissue and processed cells and BCA detection kit (Solarbio, Beijing) was used to identify protein concentration. Perform 6-15% SDS-polyacrylamide gel electrophoresis on the average amount of protein in each group. Then, the separated protein was transferred to a nitrocellulose membrane (Pall, USA) at 4°C. The membrane was blocked, and then hatched overnight with diluted primary antibodies at 4°C: NF-κB (1:500), TNF-α (1:500), iNOS (1:500), COX-2 (1:500), IL-1β (1:400), IL-6 (1:1000), IL-10 (1:500), IFN-γ (1:500), TGFβ (1:1000), α-SMA (1:1000), EGF (1:1000), bFGF (1:1000), MPO (1:500), Cit H3 (1:1000), NE (1:500), Wnt (1:750), β-catenin (1:750), GSK-3β (1:400) and β-Tubilin (1:1000). After the antibody was recovered, the membrane was washed three times in TBST and hatched with HRP-conjugated anti-rabbit and anti-mouse secondary antibodies (1:10000, Immunoway, Beijing). Finally, the ECL kit (Biosharp, China) was used to visualize the bands on the membrane in the Azure Imaging Biosystem C300.

4.10 Statistical analyses

All data were submitted to one-way analysis of variance, and the Tukey method was used for multiple comparisons. GraphPad Prism (version 9.1, USA) was used to draw graphs. The results of this experiment were shown as mean ± standard error of mean (SEM). As shown in the legend, n represents the number of replicates of a single mouse or a single experiment. We performed the Shapiro-Wilk normality test and found that the data in this article passed the normality test (alpha=0.05).

Abbreviations

Abbreviations	Full names
MPs	Microplastics
DEHP	Di-(2-ethylhexylPhthalate)
MDA	Malondialdehyde
GSH-Px	Glutathione peroxidase
GSH	Glutathione
CAT	Catalase
T-AOC	Total antioxidant capacity
CCL1, 4, 17	CC chemokine subfamily 1, 4, 17
CXCL12, 13, 14	CXC chemokine subfamily 12, 13, 14
ROS	Reactive oxygen species
Net	Neutrophil extracellular trap
MPO	Myeloperoxidase
Cit H3	Citrullinated histone H3
NE	Neutrophil elastase
PAD4	Peptidylarginine deiminase type 4
NF-κB	Nuclear factor kappa-B
TNF-α	Tumor necrosis factor-α
iNOS	Nitric Oxide Synthase
COX-2	Cyclo-oxygen-ase-2
PTGEs	Prostaglandin E synthases
IL-1β, 6, 8, 10	Interleukin-1β, 6, 8, 10
GSK-3β	Glycogen synthase kinase-3β
TGFβ	Transforming growth factor-β
α-SMA	α-smooth muscle actin
EGF	Epidermal growth factor
bFGF	Basic fibroblast growth factor
IGF-1	Insulin-like growth factors-1
KGF	Keratinocyte growth factor

PDGF	Plateletogenic growth factor
Col1, 3	Collagen 1, 3

Declarations

Ethics approval and consent to participate

All procedures were approved by the Northeast Agricultural University Animal Management and Use Committee (SRM-11).

Consent for publication

Not applicable.

Data availability statement

The datasets used and/or analyzed during the current study are available from the corresponding author upon reasonable request.

Declaration of Competing Interest

The authors declare that they have no known competing financial interests or personal relationships that could have appeared to influence the work reported in this paper.

Funding

This research did not receive any specific grant from funding agencies in the public, commercial, or not-for-profit sectors.

CRediT authorship contribution statement

Xu Shi: Formal analysis, Writing-original draft, Investigation. **Wei Cui**: Visualization. **Tong Xu**: Software, Investigation. **Xue Qi**: Investigation. **Zhiruo Miao**: Software, Investigation, Resources. **Shiwen Xu**: Conceptualization, Supervision, Validation, Writing review & editing.

Acknowledgements

Not applicable.

References

1. An, Z., J. Li, J. Yu, X. Wang, H. Gao, W. Zhang, Z. Wei, J. Zhang, Y. Zhang, J. Zhao and X. Liang (2019). "Neutrophil extracellular traps induced by IL-8 aggravate atherosclerosis via activation NF-κB signaling in macrophages." Cell cycle (Georgetown, Tex.) **18**(21): 2928-2938.

2. Camacho, L., J. Latendresse, L. Muskhelishvili, C. Law and K. Delclos (2020). "Effects of intravenous and oral di(2-ethylhexyl) phthalate (DEHP) and 20% Intralipid vehicle on neonatal rat testis, lung, liver, and kidney." Food and chemical toxicology : an international journal published for the British Industrial Biological Research Association **144**: 111497.
3. Cheng, S., R. Lv, J. Xu, A. Hirman and L. Du (2021). "IGF-1-Expressing Placenta-Derived Mesenchymal Stem Cells Promote Scalding Wound Healing." The Journal of surgical research **265**: 100-113.
4. Chi, Q., Q. Zhang, Y. Lu, Y. Zhang, S. Xu and S. Li (2021). "Roles of selenoprotein S in reactive oxygen species-dependent neutrophil extracellular trap formation induced by selenium-deficient arteritis." Redox biology **44**: 102003.
5. Cincinelli, A., C. Scopetani, D. Chelazzi, E. Lombardini, T. Martellini, A. Katsoyiannis, M. Fossi and S. Corsolini (2017). "Microplastic in the surface waters of the Ross Sea (Antarctica): Occurrence, distribution and characterization by FTIR." Chemosphere **175**: 391-400.
6. Feng, S., Y. Zeng, Z. Cai, J. Wu, L. Chan, J. Zhu and J. Zhou (2021). "Polystyrene microplastics alter the intestinal microbiota function and the hepatic metabolism status in marine medaka (Oryzias melastigma)." The Science of the total environment **759**: 143558.
7. Gao, M., Y. Xu, Y. Dong, Z. Song and Y. Liu (2019). "Accumulation and metabolism of di(n-butyl) phthalate (DBP) and di(2-ethylhexyl) phthalate (DEHP) in mature wheat tissues and their effects on detoxification and the antioxidant system in grain." The Science of the total environment **697**: 133981.
8. Gos, M., J. Miłoszewska and M. Przybyszewska (2009). "[Epithelial-mesenchymal transition in cancer progression]." Bulletin De Lacademie Nationale De Medecine **193**(2): 1969.
9. Guan, X., Y. He, Z. Wei, C. Shi, Y. Li, R. Zhao, L. Pan, Y. Han, T. Hou and J. Yang (2021). "Crosstalk between Wnt/β-catenin signaling and NF-κB signaling contributes to apical periodontitis." International immunopharmacology **98**: 107843.
10. Jiang, P., G. Yuan, B. Jiang, J. Zhang, Y. Wang, H. Lv, Z. Zhang, J. Wu, Q. Wu and L. Li (2021). "Effects of microplastics (MPs) and tributyltin (TBT) alone and in combination on bile acids and gut microbiota crosstalk in mice." Ecotoxicology and environmental safety **220**: 112345.
11. Karim, S., H. Alkreathy, A. Ahmad and M. Khan (2021). "Effects of Methanolic Extract Based-Gel From Saudi Pomegranate Peels With Enhanced Healing Potential on Excision Wounds in Diabetic Rats." Frontiers in pharmacology **12**: 704503.
12. Kim, J., J. Shin, Y. Choi, S. Lee, M. Jin, C. Kim, N. Kang and S. Lee (2021). "Adenosine and Cordycepin Accelerate Tissue Remodeling Process through Adenosine Receptor Mediated Wnt/β-Catenin Pathway Stimulation by Regulating GSK3b Activity." International journal of molecular sciences **22**(11).
13. Koongolla, J., L. Lin, Y. Pan, C. Yang, D. Sun, S. Liu, X. Xu, D. Maharana, J. Huang and H. Li (2020). "Occurrence of microplastics in gastrointestinal tracts and gills of fish from Beibu Gulf, South China Sea." Environmental pollution (Barking, Essex : 1987) **258**: 113734.

14. Lai, X., M. Wang, Y. Zhu, X. Feng, H. Liang, J. Wu, L. Nie, L. Li and L. Shao (2021). "ZnO NPs delay the recovery of psoriasis-like skin lesions through promoting nuclear translocation of p-NFκB p65 and cysteine deficiency in keratinocytes." Journal of hazardous materials **410**: 124566.
15. Lämmermann, T., P. Afonso, B. Angermann, J. Wang, W. Kastenmüller, C. Parent and R. Germain (2013). "Neutrophil swarms require LTB4 and integrins at sites of cell death in vivo." Nature **498**(7454): 371-375.
16. Li, R., J. Liang, H. Duan and Z. Gong (2017). "Spatial distribution and seasonal variation of phthalate esters in the Jiulong River estuary, Southeast China." Marine pollution bulletin **122**: 38-46.
17. Martin, P. and S. Leibovich (2005). "Inflammatory cells during wound repair: the good, the bad and the ugly." Trends in cell biology **15**(11): 599-607.
18. Mei, H., P. Yao, S. Wang, N. Li, T. Zhu, X. Chen, M. Yang, S. Zhuo, S. Chen, J. Wang, H. Wang, D. Xie, Y. Wu and Y. Le (2017). "Chronic Low-Dose Cadmium Exposure Impairs Cutaneous Wound Healing With Defective Early Inflammatory Responses After Skin Injury." Toxicological sciences : an official journal of the Society of Toxicology **159**(2): 327-338.
19. Oh, P., K. Lim and K. Lim (2010). "Phytoglycoprotein (75 kDa) inhibits expression of interleukin-1beta stimulated by DEHP in human mast cells." Cell biochemistry and function **28**(5): 352-359.
20. Papayannopoulos and Venizelos (2017). "Neutrophil extracellular traps in immunity and disease." Nature Reviews Immunology.
21. Shengchen, W., L. Jing, Y. Yujie, W. Yue and X. Shiwen (2021). "Polystyrene microplastics-induced ROS overproduction disrupts the skeletal muscle regeneration by converting myoblasts into adipocytes." Journal of hazardous materials **417**: 125962.
22. Shi, X., W. Wang, S. Zheng, Q. Zhang and S. Xu (2020). "Selenomethionine relieves inflammation in the chicken trachea caused by LPS though inhibiting the NF-κB pathway." Biological trace element research **194**(2): 525-535.
23. Song, N., X. Li, Y. Cui, T. Zhang, S. Xu and S. Li (2021). "Hydrogen sulfide exposure induces pyroptosis in the trachea of broilers via the regulatory effect of circRNA-17828/miR-6631-5p/DUSP6 crosstalk on ROS production." Journal of hazardous materials **418**: 126172.
24. Takdastan, A., M. Niari, A. Babaei, S. Dobaradaran, S. Jorfi and M. Ahmadi (2021). "Occurrence and distribution of microplastic particles and the concentration of Di 2-ethyl hexyl phthalate (DEHP) in microplastics and wastewater in the wastewater treatment plant." Journal of environmental management **280**: 111851.
25. Thomas, P., G. Perono, F. Tommasi, G. Pagano, R. Oral, P. Burić, I. Kovačić, M. Toscanesi, M. Trifuoggi and D. Lyons (2021). "Resolving the effects of environmental micro- and nanoplastics exposure in biota: A knowledge gap analysis." The Science of the total environment **780**: 146534.
26. Wang and Jing (2018). "Neutrophils in tissue injury and repair." Cell & Tissue Research.
27. Wang, J., Z. Liu, Z. Han, Z. Wei, Y. Zhang, K. Wang and Z. Yang (2020). "Fumonisin B triggers the formation of bovine neutrophil extracellular traps." Toxicology letters **332**: 140-145.

28. Wang, J., Y. Tian, M. Li, Y. Feng, L. Kong, F. Zhang and W. Shen (2021). "Single-cell transcriptome dissection of the toxic impact of Di (2-ethylhexyl) phthalate on primordial follicle assembly." Theranostics **11**(10): 4992-5009.
29. Wang, S., S. Zheng, Q. Zhang, Z. Yang, K. Yin and S. Xu (2018). "Atrazine hinders PMA-induced neutrophil extracellular traps in carp via the promotion of apoptosis and inhibition of ROS burst, autophagy and glycolysis." Environmental pollution (Barking, Essex : 1987) **243**: 282-291.
30. Wong, S., M. Demers, K. Martinod, M. Gallant, Y. Wang, A. Goldfine, C. Kahn and D. Wagner (2015). "Diabetes primes neutrophils to undergo NETosis, which impairs wound healing." Nature medicine **21**(7): 815-819.
31. Yang, H., Y. Tsai, M. Korivi, C. Chang and Y. Hseu (2017). "Lucidone Promotes the Cutaneous Wound Healing Process via Activation of the PIK/AKT, Wnt/β-catenin and NF-κB Signaling Pathways." Biochimica et biophysica acta. Molecular cell research **1864**(1): 151-168.
32. Yirong, C., W. Shengchen, S. Jiaxin, W. Shuting and Z. Ziwei (2020). "DEHP induces neutrophil extracellular traps formation and apoptosis in carp isolated from carp blood via promotion of ROS burst and autophagy." Environmental pollution (Barking, Essex : 1987) **262**: 114295.
33. Yousif, E. and R. Haddad (2013). "Photodegradation and photostabilization of polymers, especially polystyrene: review." SpringerPlus **2**: 398.
34. Zhang, C., T. Lin, G. Nie, R. Hu, S. Pi, Z. Wei, C. Wang, C. Xing and G. Hu (2021). "Cadmium and molybdenum co-induce pyroptosis via ROS/PTEN/PI3K/AKT axis in duck renal tubular epithelial cells." Environmental pollution (Barking, Essex : 1987) **272**: 116403.
35. Zhang, C., X. Wang, S. Pi, Z. Wei, C. Wang, F. Yang, G. Li, G. Nie and G. Hu (2021). "Cadmium and molybdenum co-exposure triggers autophagy via CYP450s/ROS pathway in duck renal tubular epithelial cells." The Science of the total environment **759**: 143570.
36. Zhang, E., X. Geng, S. Shan, P. Li, S. Li, W. Li, M. Yu, C. Peng, S. Wang, H. Shao and Z. Du (2021). "Exosomes derived from bone marrow mesenchymal stem cells reverse epithelial-mesenchymal transition potentially via attenuating Wnt/β-catenin signaling to alleviate silica-induced pulmonary fibrosis." Toxicology mechanisms and methods: 1-40.
37. Zhang, T., Y. Sun, K. Song, W. Du, W. Huang, Z. Gu and Z. Feng (2021). "Microplastics in different tissues of wild crabs at three important fishing grounds in China." Chemosphere **271**: 129479.
38. Zhang, X., Q. Liu, Y. Wang and H. Thorlacius (2001). "CXC chemokines, MIP-2 and KC, induce P-selectin-dependent neutrophil rolling and extravascular migration in vivo." British journal of pharmacology **133**(3): 413-421.
39. Zheng, S., S. Wang, Q. Zhang, Z. Zhang and S. Xu (2020). "Avermectin inhibits neutrophil extracellular traps release by activating PTEN demethylation to negatively regulate the PI3K-ERK pathway and reducing respiratory burst in carp." Journal of hazardous materials **389**: 121885.
40. Zhou, E., Y. Sun, Y. Fu, X. Wang, X. Zhu, Z. Wu, P. Li, J. Wang and Z. Yang (2021). "Bongkrekic acid induced neutrophil extracellular traps via p38, ERK, PAD4, and P2X1-mediated signaling." Toxicology and applied pharmacology **423**: 115580.

41. Zhu, B., X. Zhang, S. Sun, Y. Fu, L. Xie and P. Ai (2021). "NF-κB and neutrophil extracellular traps cooperate to promote breast cancer progression and metastasis." Experimental cell research **405**(2): 112707.

Figures

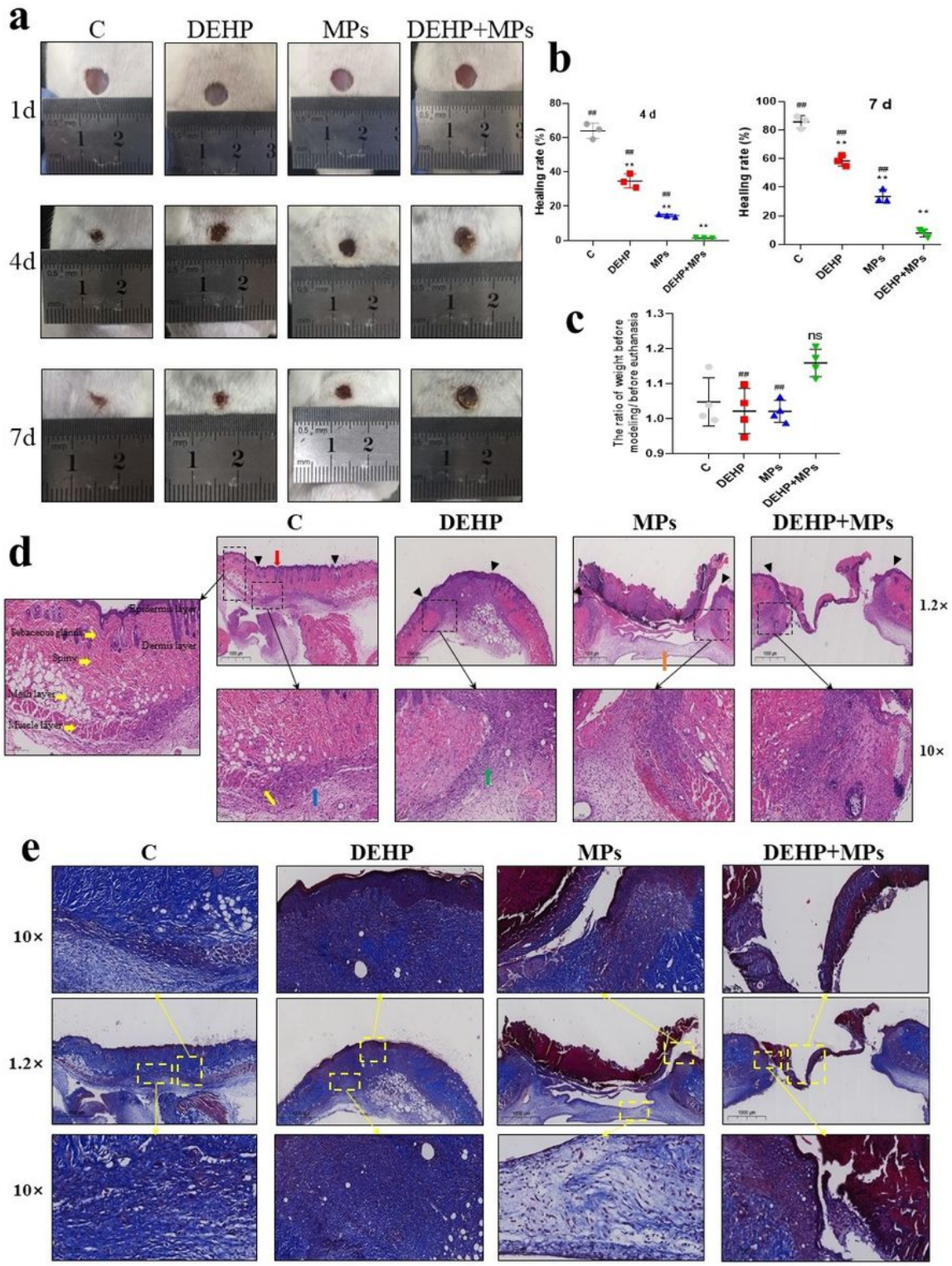

Figure 1

Effects of MPs and DEHP on wound healing (a) General view of skin wounds at designated time points (1d, 4d, and 7d) (Scale bar, 1 mm). (b) Skin wound healing rate of control group, DEHP group, MPs group and DEHP+MPs group on the 4th and 7th day (n=3). (c) The ratio of weight before skin wound modeling and before euthanasia (n=4). (d) H&E staining of skin wounds in mice. Between the black triangles is the area of the wound. The scale of low power lens (1.2×) is 1000 μm. Select the disease-health junction and magnify it to a high magnification lens (10×), with a scale of 100 μm. (e) Masson staining of skin wounds in mice. The scale of low power lens (1.2×) is 1000 μm. Select the disease-health junction and the bottom of the wound to magnify to a high magnification lens (10×), with a scale of 100 μm. "*" represents a significant difference from the control group ($p<0.05$); "#" represents a significant difference from the DEHP+MPs group ($p<0.05$).

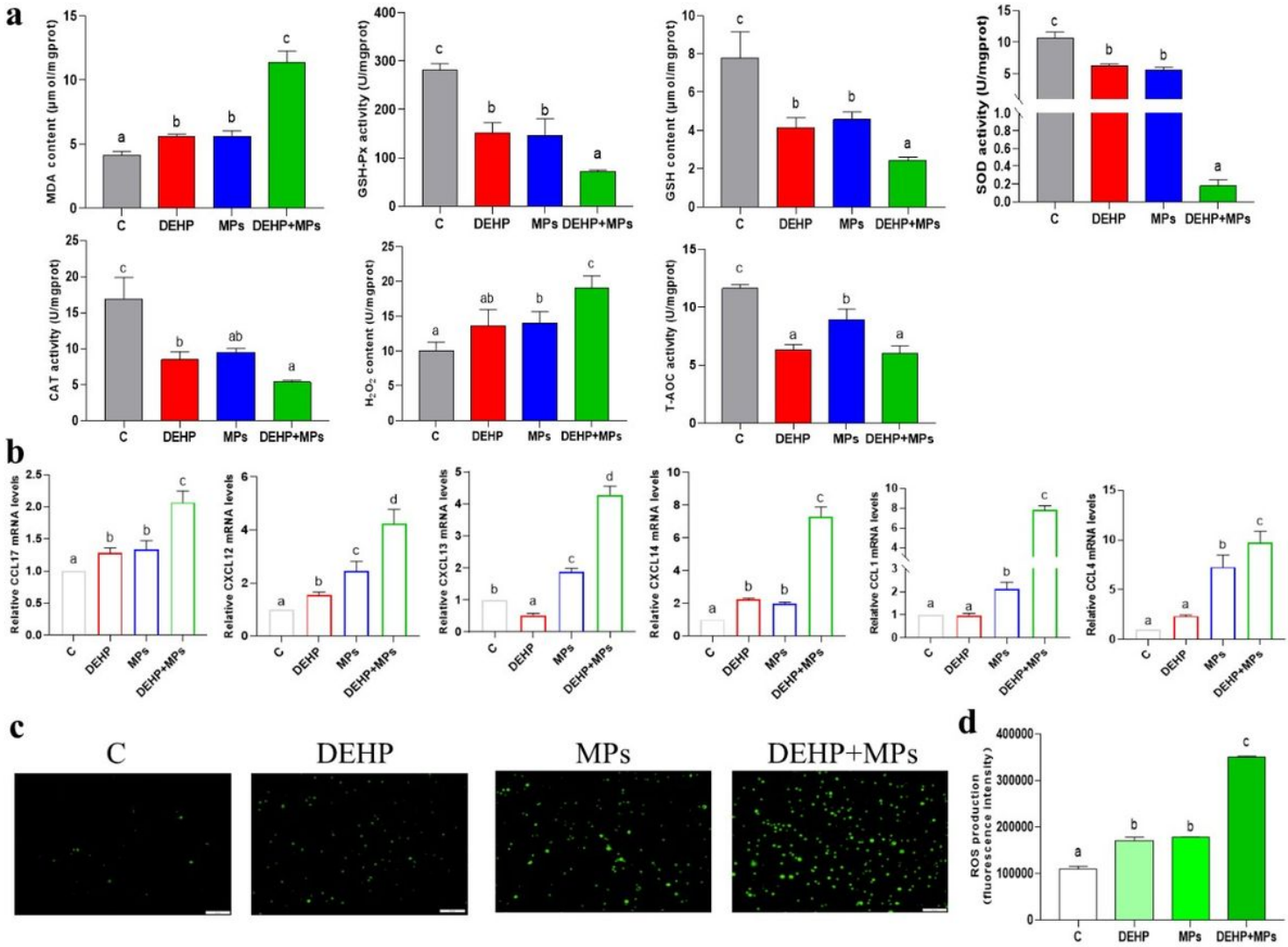

Figure 2

Effects of MPs and DEHP on oxidative stress and ROS (a) In vivo: the contents of MDA, GSH, H2O2 and the activities of GSH-Px, SOD, CAT, T-AOC in the skin wounds of mice (n=4). (b) The mRNA expression results of chemokines (CCL1, CCL4, CCL17, CXCL12, CXCL13 and CXCL14) in the skin wounds of mice (n=4). (c) The results of ROS by fluorescence microscope observation in the control group, DEHP group,

MPs group and DEHP+MPs group. (d) The result of fluorescence microplate reader detecting neutrophil ROS. The same letter represents no significant difference ($p>0.05$); completely different letters represent significant difference ($p<0.05$).

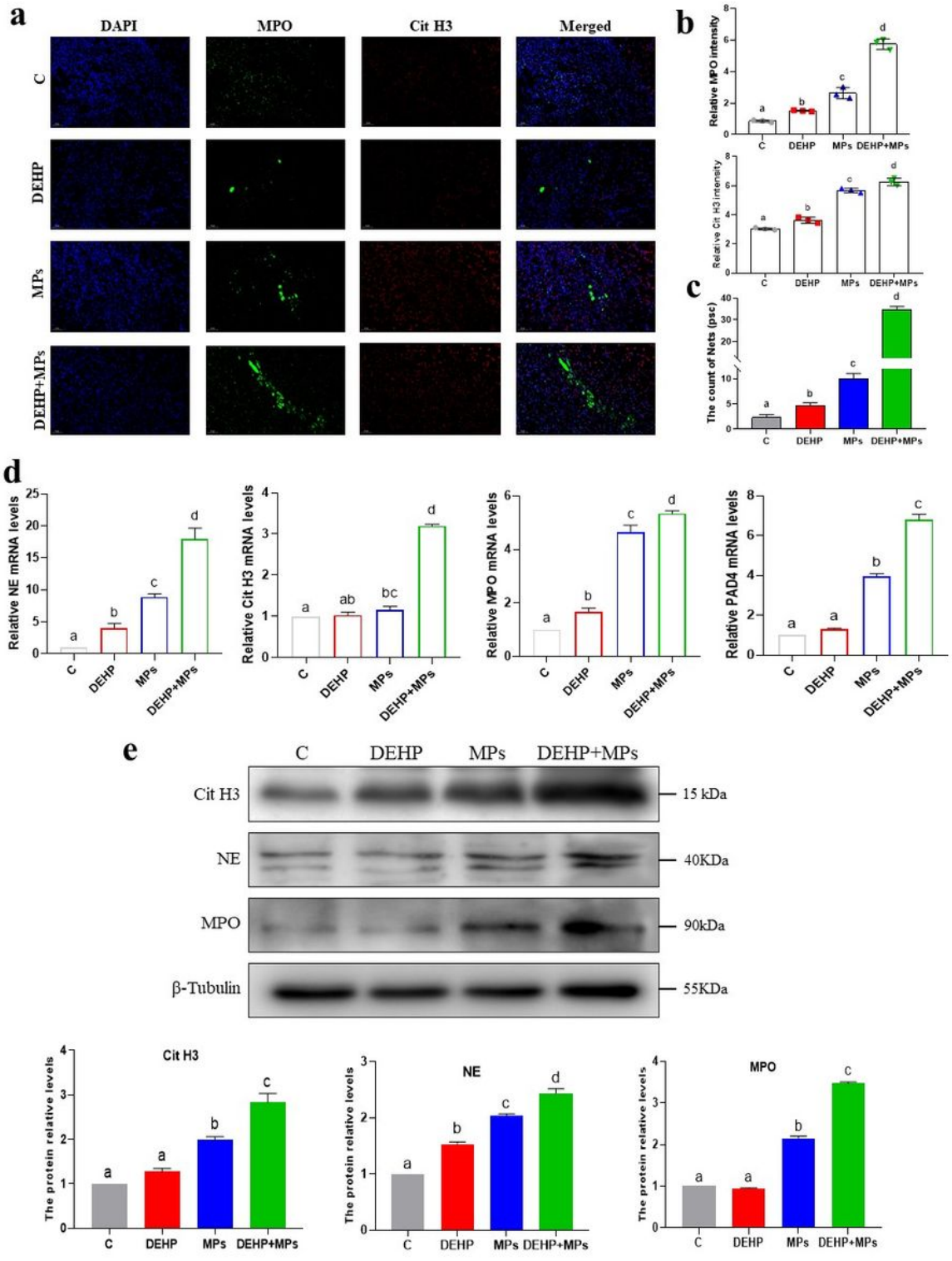

Figure 3

Effect of MPs and DEHP on the formation of Nets in wounded skin (a) The results of immunofluorescence double staining of mouse skin wound Nets markers [Cit H3 (red) and MPO (green)].

DAPI (blue) was used to stain the nucleus (scale bar, 50 μm). (b) Quantification of MPO and Cit H3 immunofluorescence images (fluorescence intensity) (n=3). (c) The count of the immunofluorescence Merged chart (Nets formation) (n=3). (d) The mRNA results of NE, Cit H3, MPO and PAD4 in mouse skin wounds (n=4). (e) The protein expression levels and quantified histograms of NE, Cit H3 and MPO in mouse skin wounds (n=3). The same letter represents no significant difference ($p>0.05$); completely different letters represent significant difference ($p<0.05$).

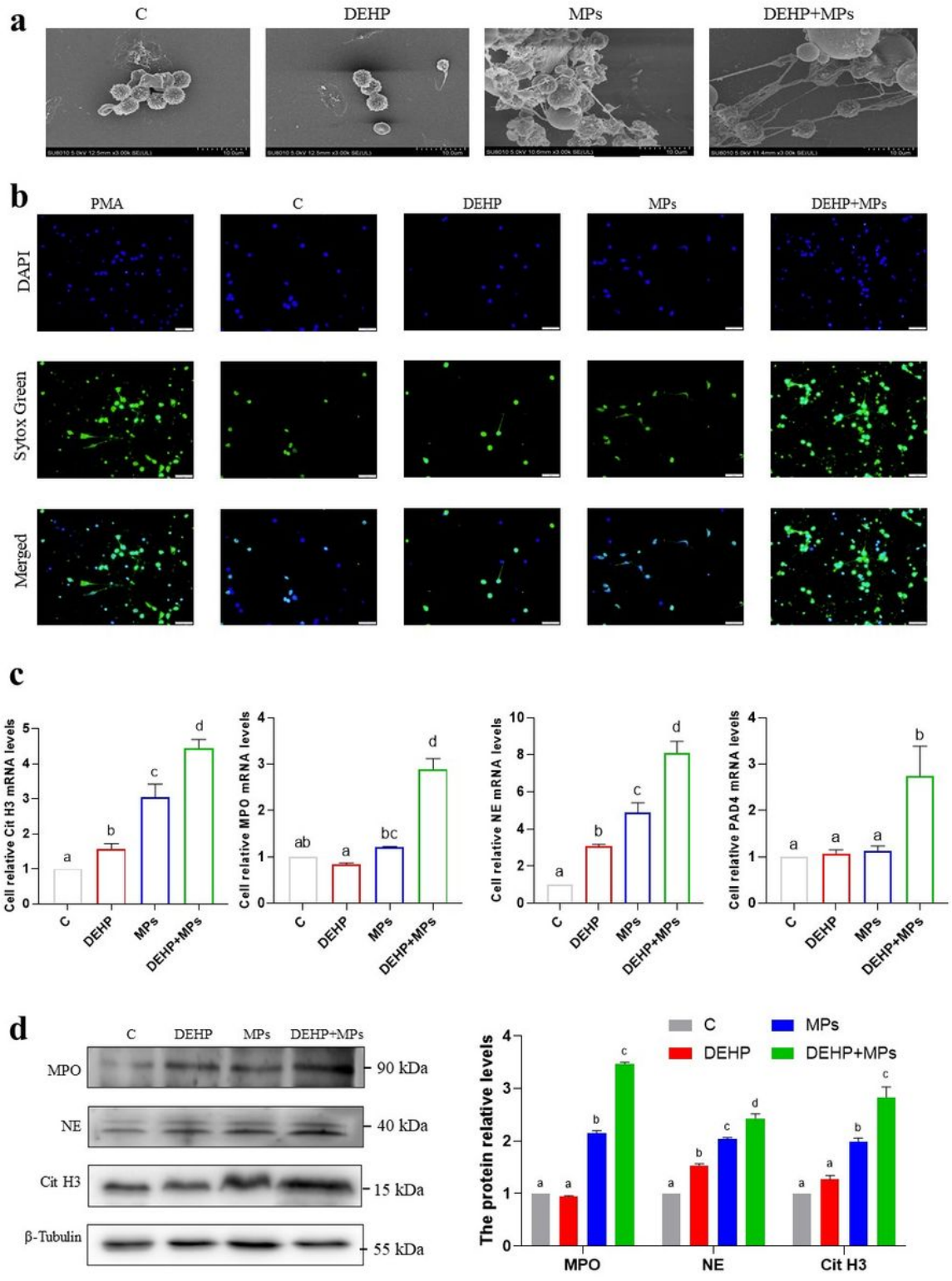

Figure 4

Effect of MPs and DEHP on the production of Nets in neutrophils (a) Scanning electron microscope to observe the results of the formation of Nets in the control group, DEHP group, MPs group and DEHP+MPs group (scale bar, 10 μm). (b) Sytox Green staining to observe the formation of Nets in the PMA group, control group, DEHP group, MPs group and DEHP+MPs group (scale bar, 50 μm). DAPI (blue) stains the nucleus. (c) In vitro, the mRNA expression results of NE, Cit H3, MPO and PAD4 in neutrophil in the control group, DEHP group, MPs group and DEHP+MPs group (n=4). (d) In vitro, the protein expression levels and quantitative graphs of NE, MPO and Cit H3 in neutrophil (n=3). The same letter represents no significant difference ($p>0.05$); completely different letters represent significant difference ($p<0.05$).

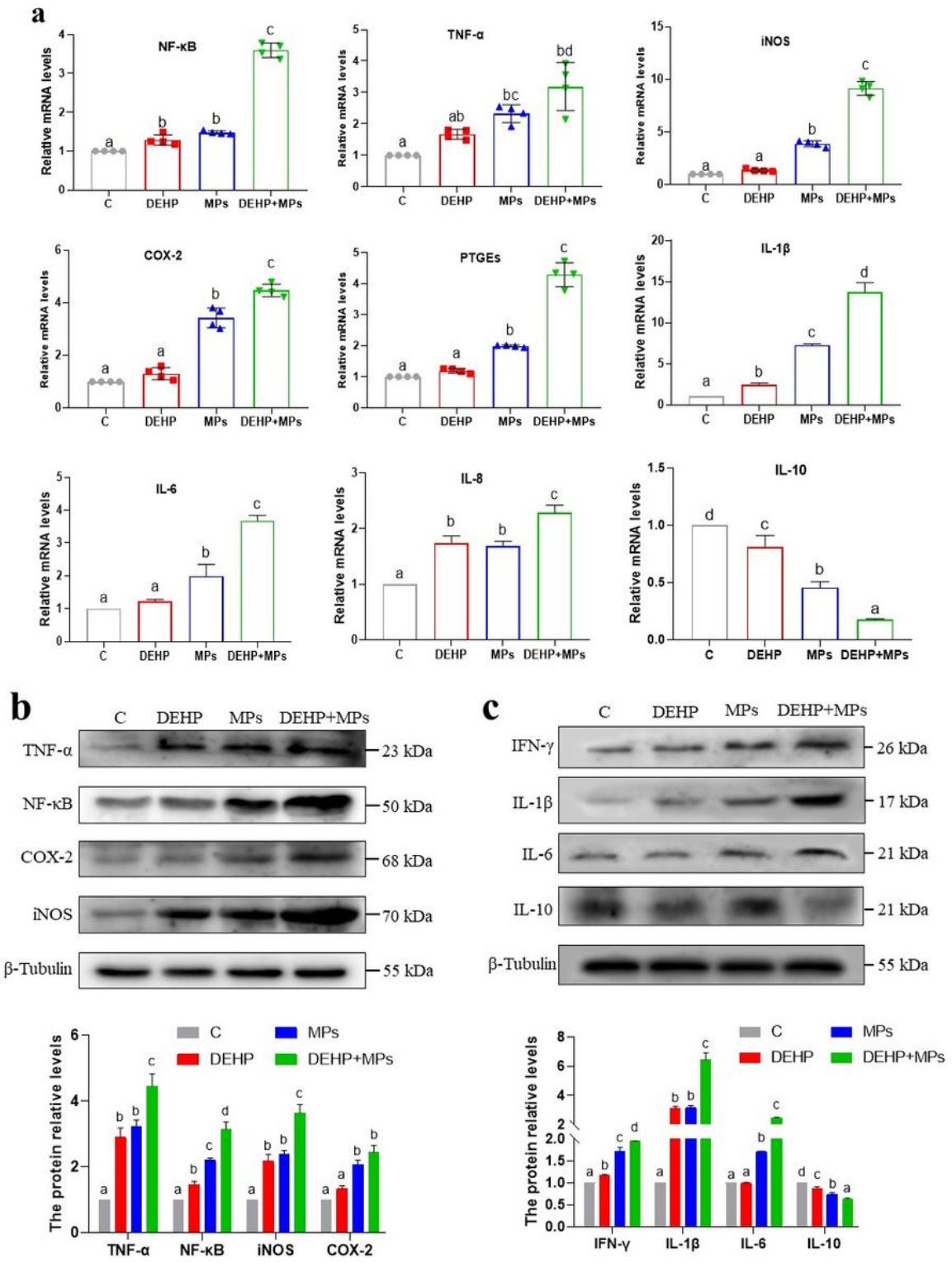

Figure 5

Effect of MPs and DEHP on skin tissue inflammation (a) The mRNA standards of NF-κB, PTGEs, TNF-α, iNOS, COX-2, IL-1β, IL-6, IL-8 and IL-10 on the skin wounds in mice (n=4). (b) The protein expression levels and quantification results of TNF-α, NF-κB, COX-2 and iNOS in mouse skin. (c) The protein expression levels and quantification results of IFN-γ, IL-1β, IL-6 and IL-10 (n=3). The same letter represents no significant difference ($p>0.05$); completely different letters represent significant difference ($p<0.05$).

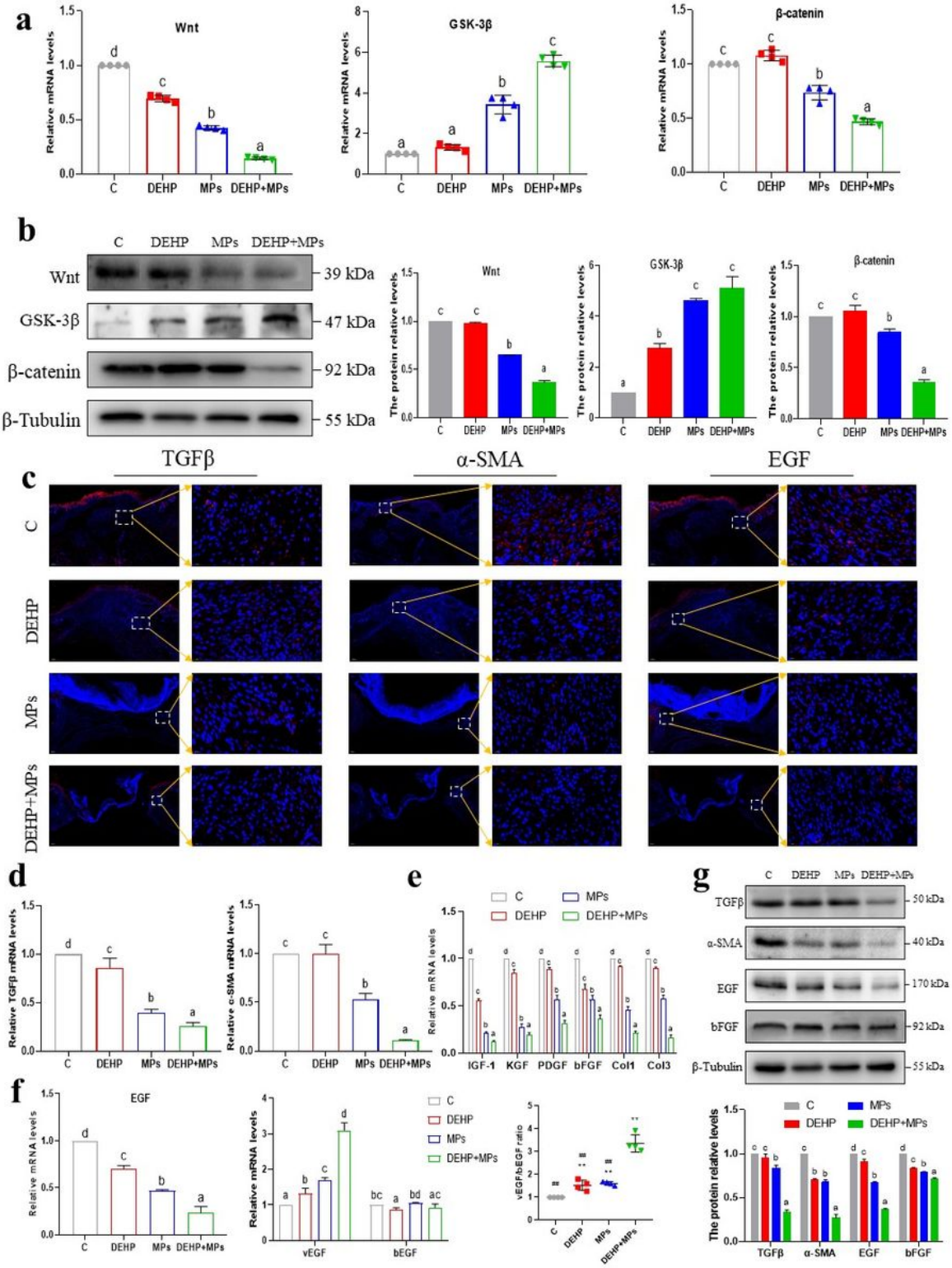

Figure 6

Effect of MPs and DEHP on Wnt, TGFβ pathways and healing factors (a) The mRNA standards of Wnt, GSK-3β and β-catenin on the skin wound in mice (n=4). (b) The protein levels and quantitative results of Wnt, GSK-3β and β-catenin (n=3). (c) The results of immunofluorescence staining of TGFβ, α-SMA and EGF (all in red) of mouse skin wounds. DAPI (blue) stains the nucleus. The scale for low-power lenses is 200 μm, and the scale for high-power lenses is 20 μm. (d) The mRNA standards of TGFβ and α-SMA on

the skin wounds in mice (n=4). (e) The mRNA levels of IGF-1, KGF, PDGF, bFGF, Col1 and Col3 in mice skin (n=4). (f) The mRNA expression levels of EGF, two types of EGF (vEGF, bEGF), and the ratio of vEGF/bEGF in the skin wounds of mice (n=4). (g) The protein levels and quantitative histograms of TGFβ, α-SMA, EGF and bFGF in the skin wounds of mice (n=3). The same letter represents no significant difference ($p>0.05$); completely different letters represent significant difference ($p<0.05$).

Supplementary Files

This is a list of supplementary files associated with this preprint. Click to download.

- GraphicalAbstract.pdf